Induced pluripotent stem cell-derived endothelial cells promote angiogenesis and accelerate wound closure in a murine excisional wound healing model

Zoë E Clayton[1, ‡], Richard P Tan[1, 2, ‡], Maria M Miravet[1,3], Katarina Lennartsson[1,3] John P Cooke[4], Christina A Bursill[1], Steven G Wise[1], Sanjay Patel[1,2] *

Word count: 5675

Brief title: IPSC-ECs promote wound healing

Disclosures: None

Author emails: zoe.clayton@sydney.edu.au; richard.tan@hri.org.au; jpcooke@houstonmethodist.org; Christina.bursill@hri.org.au; steve.wise@hri.org.au; sanjay.patel@hri.org.au

*Corresponding author

Associate Professor Sanjay Patel

Department of Cardiology

Royal Prince Alfred Hospital

50 Missenden Road, Camperdown

NSW 2050, Australia

[1]Heart Research Institute, 7 Eliza Street, Newtown, NSW 2042, Australia

[2]Sydney Medical School, University of Sydney, Camperdown, NSW 2050, Australia

[3]Linköping University, 581 83 Linköping, Sweden

[4]Department of Cardiovascular Sciences, Houston Methodist Research Institute, 6670 Bertner Ave, Houston, TX 77030, USA

[‡]ZEC and RPT contributed equally to this manuscript

[‡]ZEC and RPT contributed equally to this manuscript

Perspectives

i) Ischaemia-mediated angiogenesis is impaired in patients with cardiovascular disease and diabetes, which leads to the development of intractable wounds and ulcers.

ii) Here we show that human induced pluripotent stem cell derived endothelial cells (iPSC-ECs) promote angiogenesis, increase collagen deposition and accelerate healing in a murine wound healing model.

iii) Further development of human iPSC-ECs for therapeutic angiogenesis is a promising strategy to reduce the burden of chronic wounds in patients with peripheral arterial disease and diabetes.

Keywords

Angiogenesis, wound healing, stem cells, endothelial cells

Author Contribution Statement

ZEC and RPT contributed significantly and equally to the design and execution of this study. ZEC conceived and designed the study, developed the research plan, performed experiments, assisted with data analysis and wrote the manuscript. RPT conducted all *in vivo* and histology experiments, performed data analysis and contributed to manuscript writing. MMM and KL performed histological staining and quantitative PCR preparation and analysis. CAB provided guidance on wound healing procedures. CAB, JPC, SGW and SP supervised the project. All authors discussed the results, gave feedback and approved the final manuscript.

Abstract

Chronic wounds are a major complication in patients with cardiovascular diseases. Cell therapies have shown potential to stimulate wound healing, but clinical trials using adult stem cells have been tempered by limited numbers of cells and invasive procurement procedures. Induced pluripotent stem cells (IPSCs) have several advantages of other cell types, for example they can be generated in abundance from patients' somatic cells (autologous) or those from a matched donor. IPSCs can be efficiently differentiated to functional endothelial cells (IPSC-ECs). Here, we used a murine excisional wound model to test the pro-angiogenic properties of iPSC-ECs in wound healing. Two full-thickness wounds were made on the dorsum of NOD-SCID mice and splinted. IPSC-ECs ($5x10^5$) were topically applied to one wound, with the other serving as a control. Treatment with iPSC-ECs significantly increased wound perfusion and accelerated wound closure. Expression of endothelial cell (EC) surface marker, PECAM-1 (CD31), and pro-angiogenic EC receptor, Tie1, mRNA was upregulated in iPSC-EC treated wounds at 7 days post-wounding. Histological analysis of wound sections showed increased capillary density in iPSC-EC wounds at day 7 and day 14 post-wounding, and increased collagen content at day 14. Anti-GFP fluorescence confirmed presence of iPSC-ECs in the wounds. Bioluminescent imaging showed progressive decline of iPSC-ECs over time, suggesting that iPSC-ECs are acting primarily through short-term paracrine effects. These results highlight the pro-regenerative effects of iPSC-ECs and demonstrate that they are a promising potential therapy for intractable wounds.

Introduction

Due to poor circulation and prolonged tissue ischaemia, many patients with peripheral arterial disease develop chronic wounds or ulcers on their lower limbs, which can become infected and often necessitate amputation of the affected foot or leg. The complications associated with infection and amputation also lead to increased mortality in these patients, particularly in diabetics. Revascularisation therapies improve wound healing in patients with critical limb ischaemia, yet chronic wounds remain a major individual and societal burden, with estimated global cost of care in excess of US$22 billion each year (1, 2). Current treatments for chronic wounds are largely focused on cleaning, infection control and debridement of dead tissue. The gold-standard in chronic wound care is the split-thickness autograft, which is a patch of skin taken from a healthy region and grafted onto the wound (3). Other treatment options include bioactive dressings and donor keratinocytes, but these have limitations and additional therapies are required to better address the microvascular deficiency, which underlies the development of these wounds and contributes to their persistence and re-occurrence.

Acute wound healing is comprised of four overlapping stages; haemostasis, inflammation, proliferation and remodelling (4). The inflammation and cellular proliferation phases take place between hours to several weeks after an injury and involve the recruitment of inflammatory cells to the wound site, formation of extracellular matrix (ECM) proteins and granulation tissue, keratinocyte migration, contraction and wound closure. Angiogenesis, the growth of new blood vessel networks, is a vital component of these processes and is dependent upon pro-angiogenic growth factors released by supporting cells, proliferation and migration of local endothelial cells into the wound bed, and recruitment of bone marrow-derived stem cells/endothelial progenitor cells (EPCs) (4-7). The pathophysiology of chronic wounds is complex and disordered, but can be largely attributed to persistent inflammation and a lack of adequate tissue perfusion in the region, exacerbated by failure of ischaemia-

mediated angiogenesis in the wound. Collagen deposition is also reduced in diabetic/PAD patient wounds and the collagen that is present is often glycated, which impairs the adherence of new keratinocytes to the ECM (8). Inflammation is also known to be the primary driving force behind excessive scar formation when a wound does eventually heal (9). Meanwhile, the inability of EPCs and supporting cells to form new blood vessel networks to clear necrotic debris and deliver oxygen and nutrients to the granulation tissue maintains the wound's inflammatory status. Therapies that can effectively resolve either or both pathological processes are key to breaking the vicious cycle of failed healing in chronic wounds.

Stem cell therapy is a promising strategy to enhance angiogenesis and promote healing of chronic wounds. Adult stem and progenitor cells have been studied extensively in animal models of wound healing and appear to exert their beneficial effects via multiple mechanisms, including recruitment of other cells types, such as keratinocytes, macrophages and endothelial progenitor cells (10-12). They have also been shown to produce collagen types I and III, which are critical for regeneration of the ECM and are the source of structural integrity and tensile strength in the healing tissue (13). Clinical trials with bone marrow derived stem cells are underway and there are a handful of published studies in both acute (surgical) and chronic (venous insufficiency and diabetic) wounds, which have reported consistent decreases in wound size, particularly with repeat treatments (14-17). EPCs and embryonic stem cell derived endothelial cells have also been tested in animal models and improve wound healing via increased vascularisation (18, 19). Indeed, a common beneficial feature of all stem cell therapies seems to be their pro-angiogenic effect.

Induced pluripotent stem cells (iPSCs) are derived by reprogramming somatic cells, such as dermal fibroblasts. They have unlimited self-renewal capacity and are therefore an abundant potential source of autologous or donor matched cells for therapy and may be more clinically

translatable than other stem cell types. IPSCs can be differentiated to functional endothelial cells (iPSC-ECs) with high efficiency and reproducibility. We have shown previously that iPSC-ECs enhance angiogenesis and improve perfusion recovery in a mouse model of peripheral arterial disease (20, 21). The objective of the current study was to determine whether the pro-angiogenic properties of iPSC-ECs can be harnessed to promote wound healing. We demonstrate for the first time that iPSC-ECs enhance wound angiogenesis and perfusion, promote physiological collagen deposition and accelerate wound closure in a murine excisional wound healing model. These findings suggest that iPSC-ECs have potential as a treatment for chronic wounds and support further development of clinical grade iPSC-ECs for therapeutic angiogenesis.

Methods

IPSC reprogramming and differentiation to iPSC-ECs

Human iPSCs were generated via retroviral overexpression of Oct4, Klf4, Sox2 and c-Myc (OKSM) transcription factors in human dermal fibroblasts derived from healthy subjects. The iPSCs were differentiated to endothelial cells using previously described methods (20-23)(Supplementary figure 1). The cells were transduced with a double fusion reporter construct encoding GFP and firefly luciferase, to enable *in vivo* fluorescence and bioluminescence imaging (BLI).

Wound healing procedure

The wounding procedure was adapted from that previously described by Galiano et al. and Dunn et al. (24, 25). Male NOD/SCID mice were used at 8-10 weeks of age. The operative region of the mouse's back was prepared by removing the fur with clippers and a light depilatory cream, and two wound outlines were made, using a sterilised 5mm biopsy punch.

The skin in the middle of the outline was lifted using serrated forceps and full-thickness wounds were cut and excised using iris scissors. Silicone splints (approx. 10mm diameter) were used to prevent wound closure via contraction. An adhesive was applied sparingly to one side of the splint and the splints were centred over the wounds. The splints were then secured in place using interrupted 6-0 PROLENE™ sutures (8805H, Ethicon LLC, San Lorenzo, Puerto Rico). After splinting, the mice were scanned with a laser Doppler (MOOR-LMD V192, Moor Instruments, UK) for wound perfusion measurement. They were placed on a heat mat in the prone position and the wound area was scanned three times per mouse per timepoint. Doppler scans were performed on alternate days post-wounding, up to and including day 14. Subsequent to the initial Doppler scan, cell treatments ($5x10^5$ iPSC-ECs suspended in vehicle containing a 1:1 ratio of endothelial basal media to growth factor reduced Matrigel) were injected into the wounds and the wounds were covered with adhesive Opsite™ dressings (66000041, Smith & Nephew, London, UK). All wound healing experiments and associated procedures were conducted in accordance with National Health and Medical Research (NHMRC) guidelines for the care and use of animals for scientific purposes and were approved by the Sydney Local Health District Animal Welfare Committee, Protocol #2014-004A.

Bioluminescent imaging (BLI)

BLI was used for longitudinal tracking of iPSC-EC survival *in vivo* and was performed with an IVIS Lumina XRMS and Living Image software (Version 4.5, Perkin Elmer, Waltham, MA 02451, USA). The mice were anaesthetised with 2% isoflurane and D-luciferin (100µL, 375mg/kg) was administered by subcutaneous injection at a medial position immediately inferior to the wound sites. Bioluminescence intensity was calculated as the maximum mean

radiance (photons/second/cm^2/steradian) recorded in pre-defined regions of interest centred over the wounds. BLI was performed on alternate days post-wounding, up to and including day 14.

Histological analysis of explanted wounds

Wound explants were fixed in 4% paraformaldehyde for up to 4 hours at room temperature then changed to 70% ethanol for at least 24 hours. Paraffin infiltration was performed overnight by an automated tissue processor (Leica TP1020, Leica Biosystems Nussloch GmbH, Heidelberger Straße 17-19 69226 Nussloch, Germany). The infiltrated samples were then embedded in paraffin blocks for sectioning. Tissue samples were cut into 5 μm thick transverse sections using a rotary microtome, deparaffinised, and stained. Milligan's Trichrome stain was performed to visualise collagen content. For immunohistochemistry analysis, paraffin sections were stained using immunohistochemistry techniques with primary antibodies anti-CD31 (Abcam, USA) for endothelial cells and anti-CD68 (Abcam, USA) for macrophages. Fluorescence microscopy was then used to visualise cell markers using Alexa Fluor 594 conjugated secondary antibodies. Anti-GFP staining was done using cryosectioning. Briefly, tissue was fixed in 4% paraformaldehyde for up to 4 h at room temperature then changed to 30% sucrose for at least 24 h. Tissue was then fixed in optimum cutting temperature (OCT) compound and kept at -80^{o}C until cryosectioning. Samples were sectioned into 40 μm thick transverse sections and dropped into PBS in order for the residual O.C.T. to dissolve. Sections were then stained using standard free-floating techniques with a FITC-conjugated anti-GFP antibody (GeneTex). Both paraffin and cyrosections were then mounted and coverslipped with DAPI-containing mounting media (Vectashield, Vector Laboratories Inc., California, USA).

Analysis of host angiogenic gene expression in wounds

Total RNA was isolated from explanted control and iPSC-EC treated wounds with Trizol reagent. Real-time quantitative polymerase chain reaction analysis was performed to evaluate the expression of murine vascular endothelial cadherin (VE-cadherin; sense '5'-TCCTCTGCATCCTCACTATCACA-'3', antisense:'5'-GTAAGTGACCAACTGCTCGTGAAT-'3') , vascular endothelial growth factor receptor-1 (Flt-1; sense: '5'-GAGGAGGATGAGGGTGTCTATAGGT-'3', antisense: '5'-GTGATCAGCTCCAGGTTTGACTT-'3'), vascular endothelial growth factor receptor-2 (KDR; sense '5'- GCCCTGCTGTGGTCTCACTAC-'3', antisense: '5'-CAAAGCATTGCCCATTCGAT-'3'), platelet endothelial cell adhesion molecule (PECAM-1; sense: '5'-GAGCCCAATCACGTTTCAGTTT-'3', antisense: '5'-TCCTTCCTGCTTCTTGCTAGCT-'3'), tyrosine kinase with immunoglobulin-like and EGF-like domains-1 (Tie-1; sense: '5'- CAAGGTCACACACACGGTGAA-'3', antisense: '5'- GCCAGTCTAGGGTATTGAAGTAGGA-'3'), and vascular endothelial growth factor (VEGF; sense: '5'- TGCCAAGTGGTCCCAG-'3', antisense: '5'-GTGAGGTCTTGATCCG-'3'). Glyceraldehyde-3-phosphate dehydrogenase (GAPDH; sense: '5'- GGGGCTCTCTGCTCCTCCCTGT-'3', antisense: '5'-CGGCCAAATCCGTTCACACCGA-'3') was used as a loading control. Relative gene expression was calculated as fold change compared to paired control wounds.

Quantitative analysis of bioluminescence and histological images

Quantification of bioluminescence images was performed using LivingImage 4.5 (Perkin Elmer) software. Histological and immunohistochemical sections were imaged using a Zeiss Upright Olympus fluorescence multi-channel microscope, captured with a Nikon DP

Controller 2.2 (Olympus, Japan). Immunohistochemical and histopathological analysis was done using ImageJ. Briefly, regions of interest (ROIs) were drawn around the wound site. For endothelial cells and fibroblasts, positive staining was quantified as individual particles counted based on a common threshold intensity. All cell types were quantified from an n=6 sections per group per time point.

Statistics

Data are expressed as mean ± SEM and indicated in figures as * $p<0.05$, ** $p<0.01$. The data were compared using paired student t-tests followed by Bonferoni's post-hoc test using GraphPad Prism version 5.00 (Graphpad Software, San Diego, California) for PC. IPSC-EC experimental samples were paired to control wounds within the same mouse.

Results

Engraftment of iPSC-ECs within wounds decreases following transplantation

Bioluminescence imaging was used to quantify the levels of iPSC-EC engraftment within wounds over time. Transfection of iPSC-ECs with a dual-report construct containing both the enhanced green fluorescent protein (eGFP) and the firefly luciferase enzyme enabled visualization and quantification of transplanted iPSC-ECs. Intramuscular injection of D-luciferin substrate catalyzed a bioluminescent reaction through the firefly luciferase enzyme within viable iPSC-ECs that could be visualized and quantified using the IVIS apparatus (Figure 1A). Bioluminescence quantification over 14 days showed that iPSC-EC presence in wounds decreases steadily over time (Day 0 $1.39\text{x}10^7 \pm 5.61\text{x}10^6$ vs. Day 14 $4.04\text{x}10^4 \pm 1.53\text{x}10^4$ photons/cm^2/s/steradian). The largest decrease in bioluminescence occurred

between days 2-4 (Day 2 $8.36x10^6 \pm 5.44x10^6$ vs. Day 4 $7.66x10^5 \pm 3.65x10^5$ photons/cm^2/s/steradian, Figure 1B). Immunohistochemistry staining of the eGFP marker identified iPSC-ECs engrafted within the wound site at day 7, and a smaller proportion remaining at 14 days post-transplantation (Figure 1C).

Engraftment of iPSC-ECs correlates with upregulation of host angiogenic gene expression

Functional angiogenesis is a complex process regulated by numerous cells types and growth factors. Ischemic/injured tissues undergoing revascularization processes are often identified by the upregulation of key angiogenic genes including VE-cadherin, VEGF, Flt-1, KDR, PECAM, and Tie-1. Wounds were explanted at days 7 and 14 for qPCR analysis to determine levels of these classical angiogenic genes. Increasing trends were observed in the expression of VE-Cadherin, Flt-1, and KDR in iPSC-EC treated wounds when compared to control wounds at both time points, however no statistical significance was obtained. At day 7, PECAM and Tie-1 genes were found to be significantly upregulated by 350 ± 89% and 534 ± 134% in iPSC-EC treated wounds compared to control wounds (Figure 2). At day 14, VEGF expression was significantly upregulated by 12 ± 4% in iPSC-EC treated wounds compared to controls (Figure 2).

Wounds treated with iPSC-ECs exhibit increased angiogenesis

The anatomical hallmarks of angiogenesis include increased blood perfusion and high density of neo-capillary formation. Non-invasive infrared laser Doppler imaging was conducted at the wound sites over 14 days to visualize and quantify levels of blood perfusion for the duration of wound healing (Figure 3A). Laser Doppler analysis revealed a maximum of 2-fold increase in wound perfusion compared to control within the first 4 days following

treatment in iPSC-EC treated wounds compared to control (Figure 3B). This gradually decreased back to baseline control wound perfusion levels by day 10. The subcutaneous layers of iPSC-EC treated, and control wounds were photographed following explant. A higher density of observable blood vessels was observed in iPSC-EC treated wounds compared to control (Figure 3C). To assess neo-capillary formation, cross-sections of wound explants were stained using the CD31 endothelial cell marker. At day 7, iPSC-EC treated wounds showed a 16-fold increase in capillary density compared to control wounds, which decreased to a 4-fold increase by day 14 (Figure 3D).

IPSC-EC treatment enhances the native wound healing process

Native wound healing processes involve numerous cell phenotypes responsible for rebuilding the tissue architecture necessary for cell repopulation. Of these cell types, fibroblasts are largely implicated as essential matrix remodelling cells which facilitate neo-collagen deposition as a temporary matrix for cell growth and tissue regeneration. Using trichrome staining, wound cross-sections were quantified for levels of collagen deposition. IPSC-EC treated wounds showed a 20 ± 4% increase in collagen deposition at day 14 compared to control wounds (Figure 4B). Similar trends were observed with macrophage infiltration. At day 14, iPSC-EC treated wounds showed a 174 ± 6% increase in macrophage numbers compared to control wounds (Figure 5). The functional outcomes of wound healing were measured by taking three diameter measurements of wounds over 14 days and represented as percentage of total wound closure. IPSC-EC treated wounds show accelerated wound closure from day 2, which was significant on days 4 and 10 post-wounding and achieved complete wound closure 4 days earlier than control wounds (Figure 4A).

Discussion

Chronic wounds and ulcers persist in a state of pathological inflammation, characterised by increased proteolytic activity, increased production of reactive oxygen species (ROS), senescent or dysfunctional fibroblasts, neutrophils and macrophages, and reduced pro-angiogenic growth factors and cytokines (4, 7). The aetiology of chronic wound formation in diabetes and peripheral arterial disease is multifactorial, but a major cause is underlying vasculopathy and diminished angiogenesis. The angiogenic response to ischaemia declines naturally with age and is further impaired in patients with vascular disease, who have reduced number and functionality of circulating EPCs (26-30). The importance of angiogenesis in wound healing has been highlighted by interventional studies, which have shown that topical application of pro-angiogenic factors, such as VEGF or bFGF, is beneficial in accelerating diabetic wound healing in mice, while neutralising them has the opposite effect (31-33). However, clinical trials using single growth factors to boost angiogenesis have been largely unsuccessful, which likely reflects the complex regulation of angiogenesis *in vivo* and the need for a multifactorial approach (34).

Bone marrow and adipose tissue derived MSCs and EPCs have been in development for therapeutic angiogenesis for the past two decades, and have shown promise in promoting wound healing , however limited availability of healthy adult stem cells, and invasive aspiration procedures have tempered their use. Induced pluripotent stem cells and their derivatives have several advantages, such as their relatively abundant supply, their non-controversial origins and the lack of immunogenicity if used for autologous transplantation (35). Furthermore, the development of iPSC banking, the creation of multiple iPSC lines representing commonly present HLA allele combinations, means that patients could receive non-autologous cells without evoking an immune rejection, increasing the throughput while simultaneously reducing the time, cost and invasiveness of pluripotent cell therapies (36).

Here, we demonstrate the pro-angiogenic and wound healing capabilities of iPSC-ECs in a murine excisional wound model. Angiogenesis is vital for the formation and maintenance of granulation tissue in the first 2-4 days post wounding. Neovessel formation typically begins around this time, peaking around day 7 before giving way to remodelling and maturation of the newly formed vasculature. We observed significantly accelerated wound closure in iPSC-EC treated wounds, as well as increased wound perfusion in the first week of healing, which was associated with a significant increase in endothelial cell surface marker PECAM-1 (CD31) staining in the wounds at both 7 and 14 days post-wounding. Consistent with previously described temporal patterns of angiogenesis in wound healing, absolute laser Doppler perfusion measurements decreased in both groups during the second week, approaching the those of the surrounding healthy skin, as new dermis progressively covered exposed capillaries at the wound surface. Expression of PECAM-1 and Tie-1 mRNA was significantly upregulated in iPSC-EC wounds on day 7 but was similar to expression in control wounds by day 14. Tie 1 is an endothelial cell specific orphan receptor, which has been shown to promote sprouting angiogenesis via regulation of Tie 2 receptor signalling (37).

IPSC-EC treatment also increased wound collagen deposition; sections from wounds treated with iPSC-ECs had significantly higher collagen content than the control wounds on day 14. Collagen deposition is vital for healthy wound healing, but the implication of increased collagen depends on the stage of healing as well as the types of collagen present; in the proliferative stage of healing collagen provides a matrix to support inflammatory and vascular cells as well as forming a stronger barrier than the fibrin clot (38). In the late stages (remodelling), a reduction in collagen content is desirable to limit scarring. Collagen deposition begins within the first 24 hours after wounding and peaks between 1-3 weeks

later, depending on the wound site and size. As these wounds were still actively healing and in the proliferative phase at day 14, the observation of increased collagen is most likely indicative of a more advanced stage of healing compared to the controls, rather than excessive scarring. We also observed increased macrophage infiltration in iPSC-EC treated wounds at day 14 post-wounding, as evidenced by significantly increased CD68+ staining. In normal wound healing, macrophage infiltration peaks during the inflammatory phase (day 1-3 post-wounding) before subsiding. We observed no difference in CD68+ staining between control and iPSC-EC treated wounds at 7 days post-wounding. However, by day 14 iPSC-EC treated wounds had significantly greater CD68+ staining compared to their respective controls, suggesting sustained macrophage activity. This observation may be due to increased recruitment of macrophages in response to iPSC-ECs.

Poor cell survival and engraftment remains a major limitation to the long-term efficacy of cell therapies and therefore their suitability for clinical use. Most cells are lost within the first 48h after administration, due to poor retention and cell death due to excessive inflammation, ischaemia or anoikis, the programmed death that occurs in endothelial cells and other anchorage-dependent cell types when they lose their interaction with an extracellular matrix (39). Very few previous wound healing studies included longitudinal tracking of the implanted cells to determine their eventual fate and those that did reported low rates of engraftment (40, 41). We used a firefly luciferase reporter gene construct and BLI for longitudinal tracking of iPSC-EC survival *in vivo* and although iPSC-EC fluorescent and bioluminescent signal was still detectable in the wounds 14 days post-treatment, we observed a substantial and progressive decline over the two-week period. This data is consistent with previous *in vivo* survival of iPSC-ECs and suggests that the pro-angiogenic and pro-healing effects of our cells were primarily mediated via secretion of paracrine factors rather than engraftment or proliferation of the cells themselves (42). Despite low rates of engraftment,

stem cell treatments consistently evoke a beneficial response. This suggests that even small increases in retention could translate to sizeable improvements in tissue regeneration and long-term recovery and we are conducting further studies seeding iPSC-ECs on biomaterial scaffolds to determine if this can increase their *in vivo* longevity and potentiate their beneficial effects.

Limitations

NOD/SCID mice are widely used in human haematopoietic cell studies and are an ideal strain for human cell transplantation because they lack functional B and T lymphocytes, lack the ability to mount an antibody mediated response, and additional deficiencies in their innate immune system allow for increased donor cell engraftment (43). However, the blunted immune response to the cells creates a somewhat artificial environment in comparison to the situation in an immune competent organism. That being said, it is not possible to conduct pre-clinical, mechanistic investigations using human cells in other species without modulating the immune response. It is anticipated that the use of autologous or donor matched cells clinically would also mitigate the effects of immune rejection of the engrafted cells by the recipient, therefore we considered the NOD/SCID mouse to be the most suitable and appropriate model for these studies. It should also be noted that these mice are neither aged nor diabetic, so most innate wound healing capabilities are intact. This means that treatment effects are more difficult to detect, thus we anticipate an even more pronounced improvement after iPSC-EC treatment if we were able to use these cells in such a model.

Finally, we acknowledge that the iPSC-ECs used in this study were differentiated from iPSCs that were generated using integrating viral vectors. These cells may not be suitable for use in a clinical setting because of the possibility of foreign DNA integrating into the host genome.

However, the development of reprogramming protocols using small molecules means that iPSC-ECs for clinical applications can be generated without the use of viral vectors.

Conclusions

In this study, we have demonstrated for the first time that human iPSC-ECs have pro-angiogenic functionality in wound healing, promote fibroblast infiltration and collagen deposition, and accelerate wound closure. Longitudinal tracking of iPSC-ECs *in vivo* revealed a progressive decline in surviving iPSC-ECs over time, indicating that the cells are acting primarily through short-term paracrine effects. These findings have provoked further studies optimising iPSC-EC delivery to improve *in vivo* survival and engraftment rates, and also make a strong case for the development of clinical grade induced pluripotent stem cells and their derivatives for therapeutic angiogenesis in patients with vascular diseases.

Funding Sources

SP was supported by a National Health and Medical Research Council (NHMRC) Early Career Fellowship (grant number GNT0633283). The study was funded by the Sydney Medical School Foundation.

1. Leavitt T, Hu MS, Marshall CD, Barnes LA, Longaker MT, Lorenz HP. Stem cells and chronic wound healing: state of the art. Chronic Wound Care Management and Research. 2016;3:7-27.

2. Hinchliffe RJ, Brownrigg JRW, Andros G, Apelqvist J, Boyko EJ, Fitridge R, et al. Effectiveness of revascularization of the ulcerated foot in patients with diabetes and peripheral artery disease: a systematic review. Diabetes/Metabolism Research and Reviews. 2016;32:136-44.

405 3. Dreifke MB, Jayasuriya AA, Jayasuriya AC. Current wound healing procedures and
406 potential care. Materials science & engineering C, Materials for biological applications.
407 2015;48:651-62.
408 4. Greaves NS, Ashcroft KJ, Baguneid M, Bayat A. Current understanding of molecular
409 and cellular mechanisms in fibroplasia and angiogenesis during acute wound healing. Journal
410 of Dermatological Science. 2013;72(3):206-17.
411 5. Asahara T, Masuda H, Takahashi T, Kalka C, Pastore C, Silver M, et al. Bone
412 Marrow Origin of Endothelial Progenitor Cells Responsible for Postnatal Vasculogenesis in
413 Physiological and Pathological Neovascularization. Circulation research. 1999;85(3):221-8.
414 6. Ishida Y, Kimura A, Kuninaka Y, Inui M, Matsushima K, Mukaida N, et al. Pivotal
415 role of the CCL5/CCR5 interaction for recruitment of endothelial progenitor cells in mouse
416 wound healing. The Journal of Clinical Investigation.122(2):711-21.
417 7. Falanga V. Wound healing and its impairment in the diabetic foot. The
418 Lancet.366(9498):1736-43.
419 8. Schultz GS, Wysocki A. Interactions between extracellular matrix and growth factors
420 in wound healing. Wound Repair and Regeneration. 2009;17(2):153-62.
421 9. Martin P, Nunan R. Cellular and molecular mechanisms of repair in acute and chronic
422 wound healing. British Journal of Dermatology. 2015;173(2):370-8.
423 10. Kim S-W, Zhang H-Z, Guo L, Kim J-M, Kim MH. Amniotic Mesenchymal Stem
424 Cells Enhance Wound Healing in Diabetic NOD/SCID Mice through High Angiogenic and
425 Engraftment Capabilities. PloS one. 2012;7(7):e41105.
426 11. Jackson WM, Nesti LJ, Tuan RS. Concise Review: Clinical Translation of Wound
427 Healing Therapies Based on Mesenchymal Stem Cells. Stem Cells Translational Medicine.
428 2012;1(1):44-50.

12. Nie C, Yang D, Xu J, Si Z, Jin X, Zhang J. Locally Administered Adipose-Derived Stem Cells Accelerate Wound Healing Through Differentiation and Vasculogenesis. Cell Transplantation. 2011;20(2):205-16.

13. Fathke C, Wilson L, Hutter J, Kapoor V, Smith A, Hocking A, et al. Contribution of Bone Marrow–Derived Cells to Skin: Collagen Deposition and Wound Repair. Stem cells. 2004;22(5):812-22.

14. Badiavas EV, Falanga V. Treatment of chronic wounds with bone marrow–derived cells. Archives of Dermatology. 2003;139(4):510-6.

15. Dash NR, Dash SN, Routray P, Mohapatra S, Mohapatra PC. Targeting Nonhealing Ulcers of Lower Extremity in Human Through Autologous Bone Marrow-Derived Mesenchymal Stem Cells. Rejuvenation Research. 2009;12(5):359-66.

16. Isakson M, de Blacam C, Whelan D, McArdle A, Clover AJP. Mesenchymal Stem Cells and Cutaneous Wound Healing: Current Evidence and Future Potential. Stem Cells International. 2015;2015:831095.

17. Marino G, Moraci M, Armenia E, Orabona C, Sergio R, De Sena G, et al. Therapy with autologous adipose-derived regenerative cells for the care of chronic ulcer of lower limbs in patients with peripheral arterial disease. Journal of Surgical Research. 2013;185(1):36-44.

18. Asai J, Takenaka H, Ii M, Asahi M, Kishimoto S, Katoh N, et al. Topical application of ex vivo expanded endothelial progenitor cells promotes vascularisation and wound healing in diabetic mice. International Wound Journal. 2013;10(5):527-33.

19. Park S-J, Moon S-H, Lee H-J, Lim J-J, Kim J-M, Seo J, et al. A comparison of human cord blood- and embryonic stem cell-derived endothelial progenitor cells in the treatment of chronic wounds. Biomaterials. 2013;34(4):995-1003.

20. Rufaihah AJ, Huang NF, Jame S, Lee JC, Nguyen HN, Byers B, et al. Endothelial cells derived from human iPSCS increase capillary density and improve perfusion in a mouse model of peripheral arterial disease. Arteriosclerosis, thrombosis, and vascular biology. 2011;31(11):e72-9.

21. Clayton ZE, Yuen GS, Sadeghipour S, Hywood JD, Wong JW, Huang NF, et al. A comparison of the pro-angiogenic potential of human induced pluripotent stem cell derived endothelial cells and induced endothelial cells in a murine model of peripheral arterial disease. Int J Cardiol. 2017;234:81-9.

22. Takahashi K, Tanabe K, Ohnuki M, Narita M, Ichisaka T, Tomoda K, et al. Induction of Pluripotent Stem Cells from Adult Human Fibroblasts by Defined Factors. Cell. 2007;131(5):861-72.

23. Rufaihah AJ, Huang NF, Kim J, Herold J, Volz KS, Park TS, et al. Human induced pluripotent stem cell-derived endothelial cells exhibit functional heterogeneity. American Journal of Translational Research. 2013;5(1):21-35.

24. Galiano RD, Michaels VJ, Dobryansky M, Levine JP, Gurtner GC. Quantitative and reproducible murine model of excisional wound healing. Wound Repair and Regeneration. 2004;12(4):485-92.

25. Dunn L, Prosser HCG, Tan JTM, Vanags LZ, Ng MKC, Bursill CA. Murine Model of Wound Healing. 2013(75):e50265.

26. Loh SA, Chang EI, Galvez MG, Thangarajah H, El-ftesi S, Vial IN, et al. SDF-1α Expression during Wound Healing in the Aged Is HIF Dependent. Plastic and Reconstructive Surgery. 2009;123(2S):65S-75S.

27. Takahashi T, Kalka C, Masuda H, Chen D, Silver M, Kearney M, et al. Ischemia- and cytokine-induced mobilization of bone marrow-derived endothelial progenitor cells for neovascularization. Nature medicine. 1999;5(4):434-8.

478 28. Shintani S, Murohara T, Ikeda H, Ueno T, Honma T, Katoh A, et al. Mobilization of
479 Endothelial Progenitor Cells in Patients With Acute Myocardial Infarction. Circulation.
480 2001;103(23):2776-9.
481 29. Vasa M, Fichtlscherer S, Aicher A, Adler K, Urbich C, Martin H, et al. Number and
482 Migratory Activity of Circulating Endothelial Progenitor Cells Inversely Correlate With Risk
483 Factors for Coronary Artery Disease. Circulation research. 2001;89(1):e1-e7.
484 30. Schmidt-Lucke C, Rössig L, Fichtlscherer S, Vasa M, Britten M, Kämper U, et al.
485 Reduced Number of Circulating Endothelial Progenitor Cells Predicts Future Cardiovascular
486 Events: Proof of Concept for the Clinical Importance of Endogenous Vascular Repair.
487 Circulation. 2005;111(22):2981-7.
488 31. Galiano RD, Tepper OM, Pelo CR, Bhatt KA, Callaghan M, Bastidas N, et al. Topical
489 Vascular Endothelial Growth Factor Accelerates Diabetic Wound Healing through Increased
490 Angiogenesis and by Mobilizing and Recruiting Bone Marrow-Derived Cells. The American
491 Journal of Pathology. 2004;164(6):1935-47.
492 32. Gurtner GC, Werner S, Barrandon Y, Longaker MT. Wound repair and regeneration.
493 Nature. 2008;453(7193):314-21.
494 33. Yoshida S, Yamaguchi Y, Itami S, Yoshikawa K, Tabata Y, Matsumoto K, et al.
495 Neutralization of Hepatocyte Growth Factor Leads to Retarded Cutaneous Wound Healing
496 Associated with Decreased Neovascularization and Granulation Tissue Formation. Journal of
497 Investigative Dermatology. 2003;120(2):335-43.
498 34. Henry TD, Annex BH, McKendall GR, Azrin MA, Lopez JJ, Giordano FJ, et al. The
499 VIVA Trial: Vascular Endothelial Growth Factor in Ischemia for Vascular Angiogenesis.
500 Circulation. 2003;107(10):1359-65.
501 35. Leeper NJ, Hunter AL, Cooke JP. Stem cell therapy for vascular regeneration: adult,
502 embryonic, and induced pluripotent stem cells. Circulation. 2010;122(5):517-26.

503 36. Solomon S, Pitossi F, Rao MS. Banking on iPSC- Is it Doable and is it Worthwhile.
504 Stem Cell Rev and Rep. 2015;11(1):1-10.
505 37. Chong JJH, Reinecke H, Iwata M, Torok-Storb B, Stempien-Otero A, Murry CE.
506 Progenitor Cells Identified by PDGFR-Alpha Expression in the Developing and Diseased
507 Human Heart. Stem Cells and Development. 2013;22(13):1932-43.
508 38. Martin P. Wound healing–aiming for perfect skin regeneration. Science. 1997;276.
509 39. Li X, Tamama K, Xie X, Guan J. Improving Cell Engraftment in Cardiac Stem Cell
510 Therapy. Stem Cells International. 2016;2016:11.
511 40. Wu Y, Chen L, Scott PG, Tredget EE. Mesenchymal Stem Cells Enhance Wound
512 Healing Through Differentiation and Angiogenesis. Stem cells. 2007;25(10):2648-59.
513 41. Lee KB, Choi J, Cho SB, Chung JY, Moon ES, Kim NS. Topical embryonic stem
514 cells enhance wound healing in diabetic rats. J Orthop Res. 2011;29.
515 42. Park S-R, Kim J-W, Jun H-S, Roh JY, Lee H-Y, Hong I-S. Stem Cell Secretome and
516 Its Effect on Cellular Mechanisms Relevant to Wound Healing. Molecular Therapy.
517 2018;26(2):606-17.
518 43. Shultz LD, Ishikawa F, Greiner DL. Humanized mice in translational biomedical
519 research. Nat Rev Immunol. 2007;7(2):118-30.

520 **Figure titles and legends**

521 Figure 1. IPSC-EC engraftment in wounds. IPSC-ECs were transduced with a double fusion
522 reporter construct encoding GFP for fluorescence imaging and firefly luciferase for
523 bioluminescent imaging. A. Representative IVIS images, showing bioluminescent signal
524 present in iPSC-EC-treated wounds (right) on days 0, 6 and 14 post-wounding. B. Declining
525 bioluminescent signal in wounds over time, relative to control wound background signal. C.
526 GFP staining (green) with DAPI nuclear stain (blue) in control and iPSC-EC treated wounds
527 at on days 7 and 14 post-wounding (n=6 per treatment group).

Figure 2. IPSC-EC treatment increases expression of pro-angiogenic genes. QPCR analysis of wound mRNA revealed a significant upregulation of PECAM (CD31) and endothelial cell receptor, Tie-1, expression in iPSC-EC wounds on day 7 post wounding. This resolved by day 14. No significant differences in endothelial cell surface marker VE-Cadherin (CD144), VEGF, VEGF receptor 1 (Flt1) or VEGF receptor 2 (KDR) expression were measured. (*$p<0.05$ compared to controls, n=6 per treatment group)

Figure 3. IPSC-EC treatment increases vascular density and wound perfusion. A. Representative laser Doppler images, showing perfusion in control and iPSC-EC treated wounds on days 0, 4, 8 and 18 post-wounding. B. Wound perfusion in iPSC-EC treated wounds, relative to their respective control wounds. Increased perfusion in iPSC-EC treated wounds was most pronounced during the first week of healing. C. Representative photomicrographs of wounds, showing increased neovessel formation in iPSC-EC wounds relative to controls. D. Capillary density, as measured by CD31+ staining, was significantly increased in iPSC-EC wounds at both early and late timepoints. (*$p<0.05$, n=6 per treatment group)

Figure 4. IPSC-EC treatment increases collagen deposition and accelerates wound closure. A. Representative photomicrographs, showing progressive wound closure over a 14 day period. Rate of closure was significantly increased in iPSC-EC treated wounds compared to controls. B. Milligan's Trichrome staining for collagen content. No differences were observed on day 7; by day 14 iPSC-EC treated wounds had significantly higher collagen content. ($p<0.05$, n=6 per treatment group)

Figure 5. IPSC-EC treatment increases macrophage infiltration A. Anti-CD68 staining for macrophage infiltration. No differences were observed on day 7; by day 14 iPSC-EC treated wounds had significantly macrophage infiltration. ($p<0.05$, n=6 per treatment group)

552 Supplementary figure 1. Generation of induced pluripotent stem (iPSCs) and induced
553 pluripotent stem cell derived endothelial cells (iPSC-ECs) from dermal fibroblasts was
554 achieved by retroviral overexpression of Oct4, Sox2, Klf4 and cMyc, followed by culture in
555 endothelial lineage specific growth factors.

556

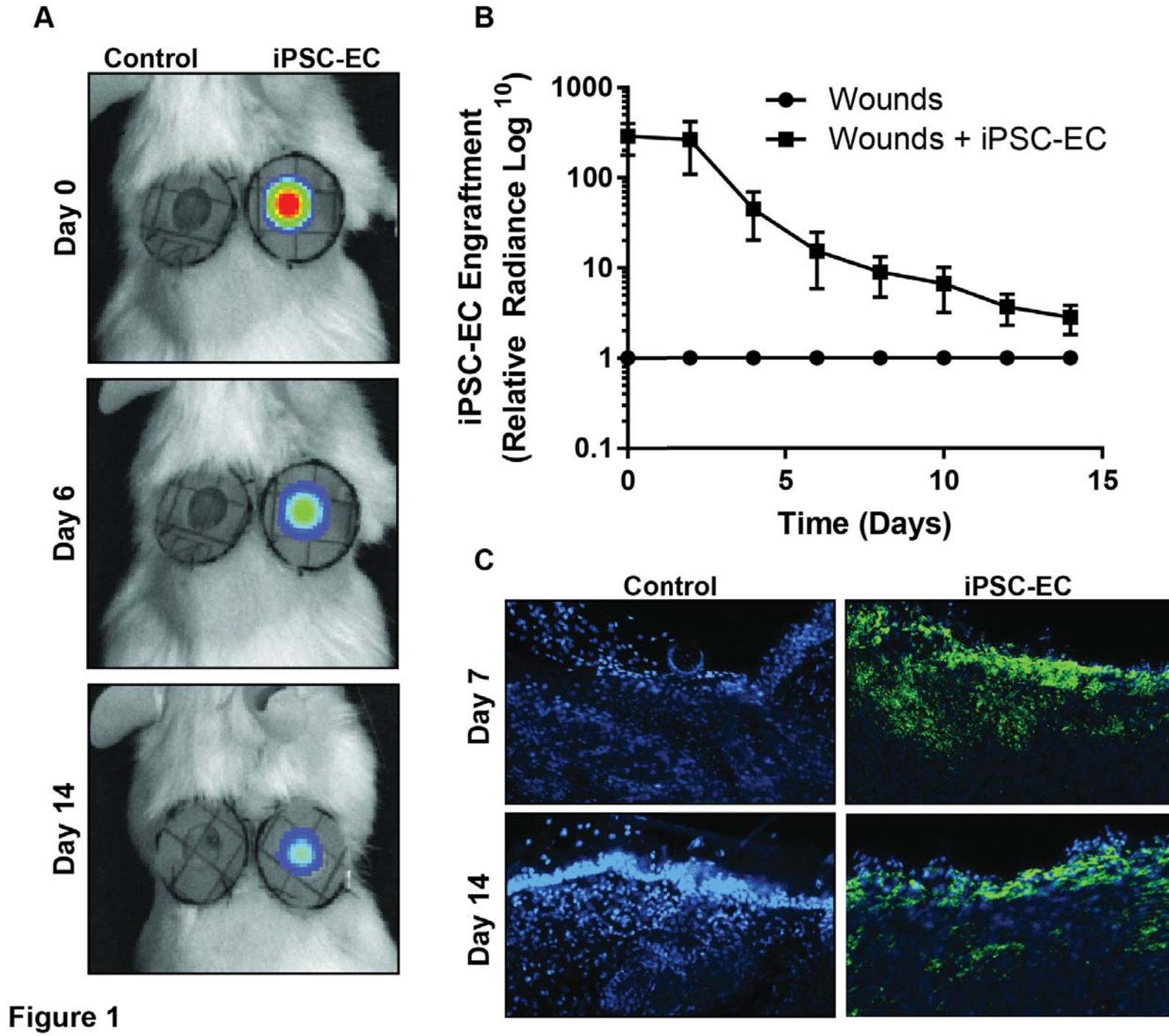
A
Control
iPSC-EC
Day 0
Day 6
Day 14
B
iPSC-EC Engraftment
(Relative Radiance Log 10)
1000
100
10
1
0.1
0
5
10
15
Time (Days)
Wounds
Wounds + iPSC-EC
C
Control
iPSC-EC
Day 7
Day 14

Figure 1

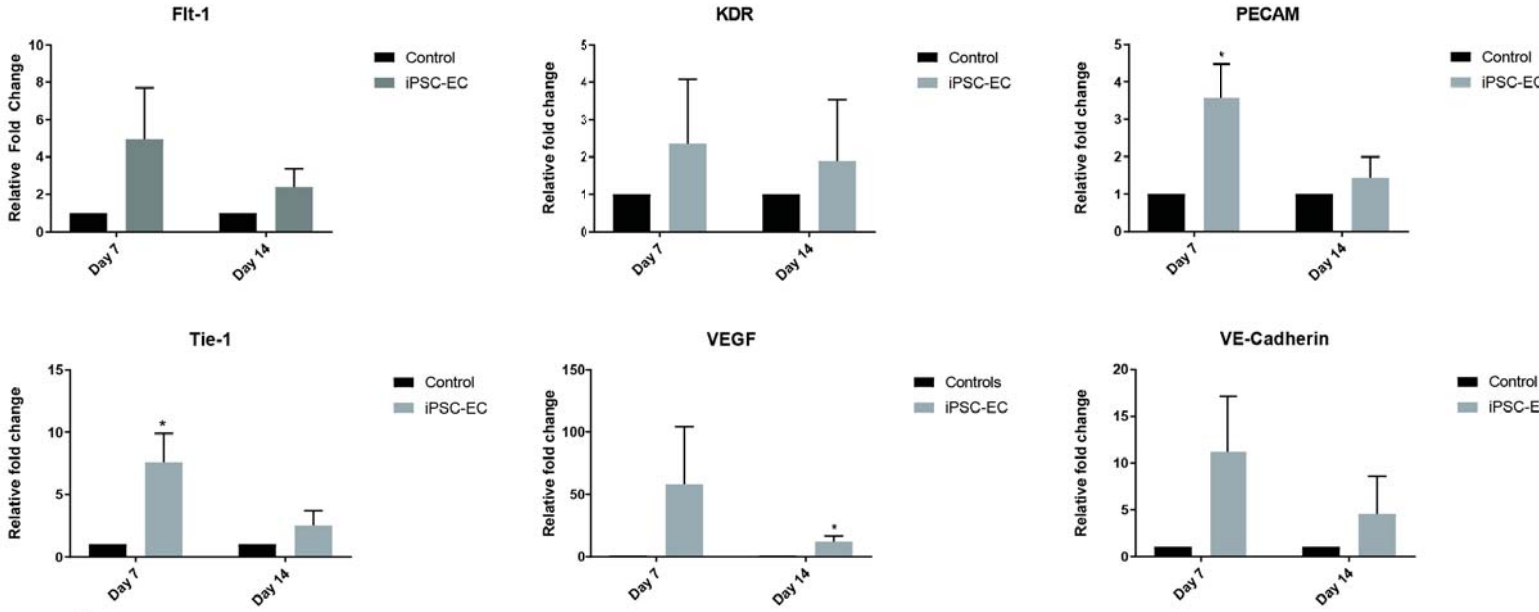
Flt-1
Relative Fold Change
Control
iPSC-EC
Day 7
Day 14
KDR
Relative fold change
Control
iPSC-EC
Day 7
Day 14
PECAM
Relative fold change
Control
iPSC-EC
Day 7
Day 14
Tie-1
Relative fold change
Control
iPSC-EC
Day 7
Day 14
VEGF
Relative fold change
Controls
iPSC-EC
Day 7
Day 14
VE-Cadherin
Relative fold change
Control
iPSC-E
Day 7
Day 14

Figure 2

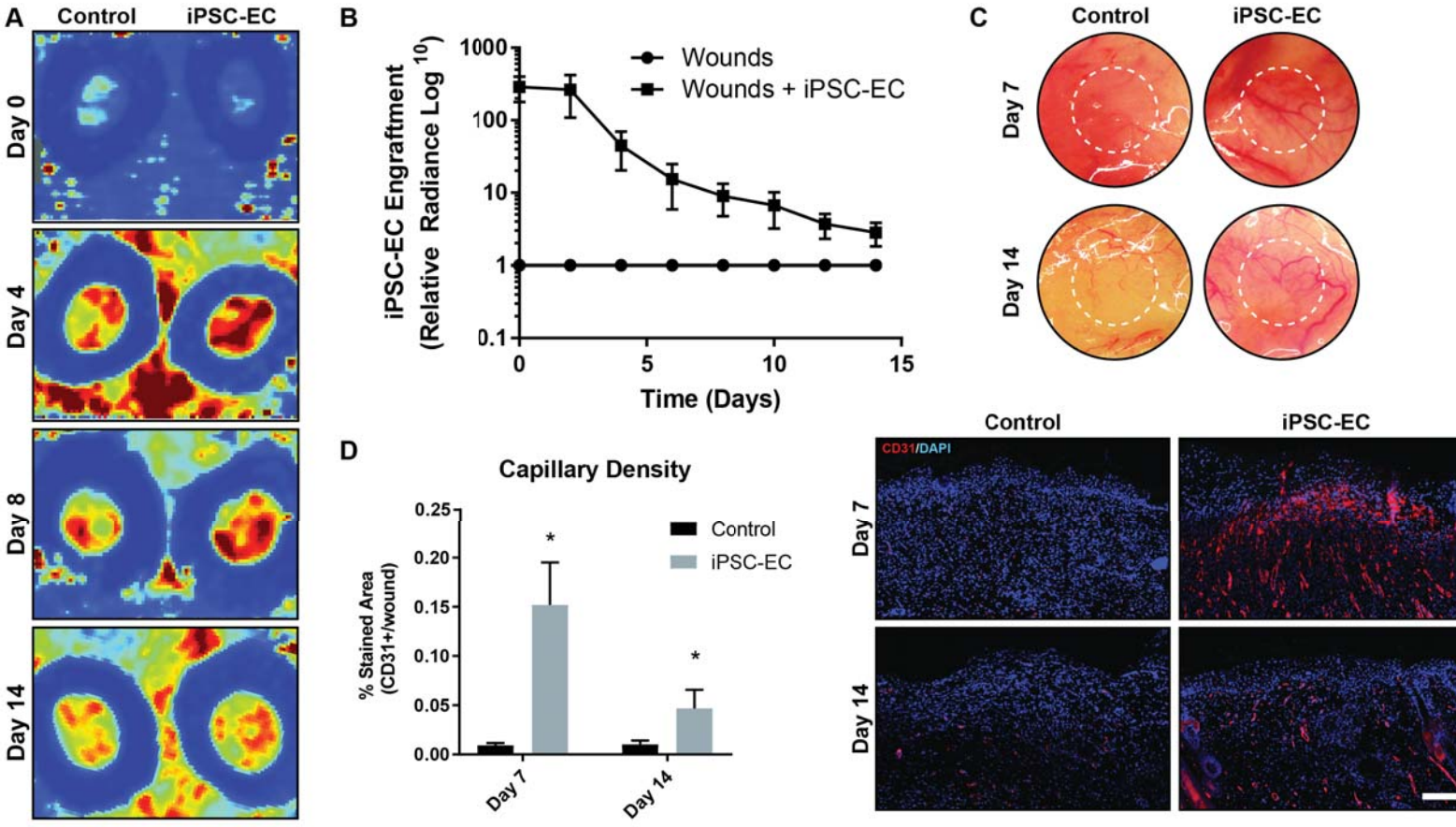
A
Control
iPSC-EC
Day 0
Day 4
Day 8
Day 14
B
iPSC-EC Engraftment (Relative Radiance Log 10)
1000
100
10
1
0.1
0
5
10
15
Time (Days)
Wounds
Wounds + iPSC-EC
C
Control
iPSC-EC
Day 7
Day 14
D
Capillary Density
% Stained Area (CD31+/wound)
0.25
0.20
0.15
0.10
0.05
0.00
Control
iPSC-EC
*
*
Day 7
Day 14
Control
iPSC-EC
CD31/DAPI
Day 7
Day 14

Figure 3

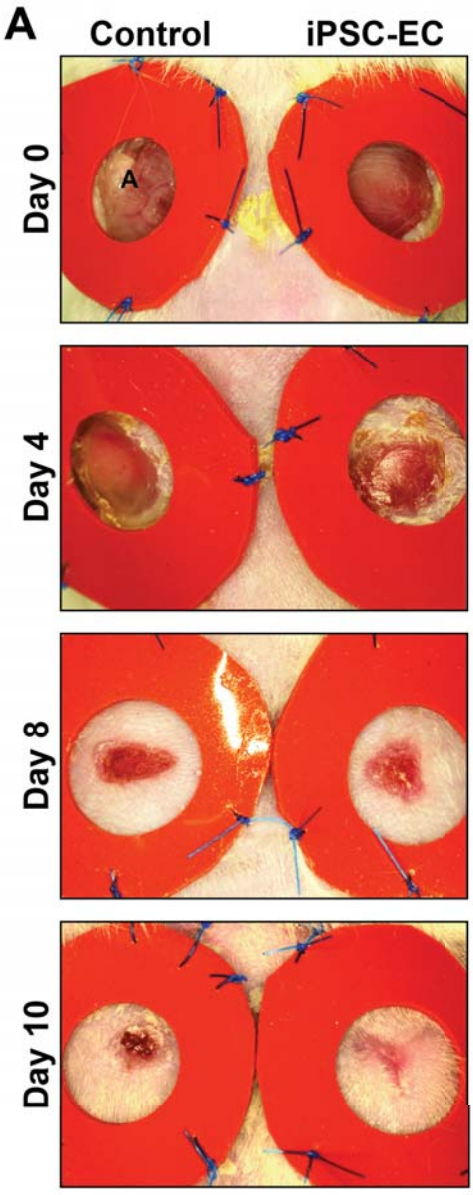
A
Control
iPSC-EC
Day 0
Day 4
Day 8
Day 10

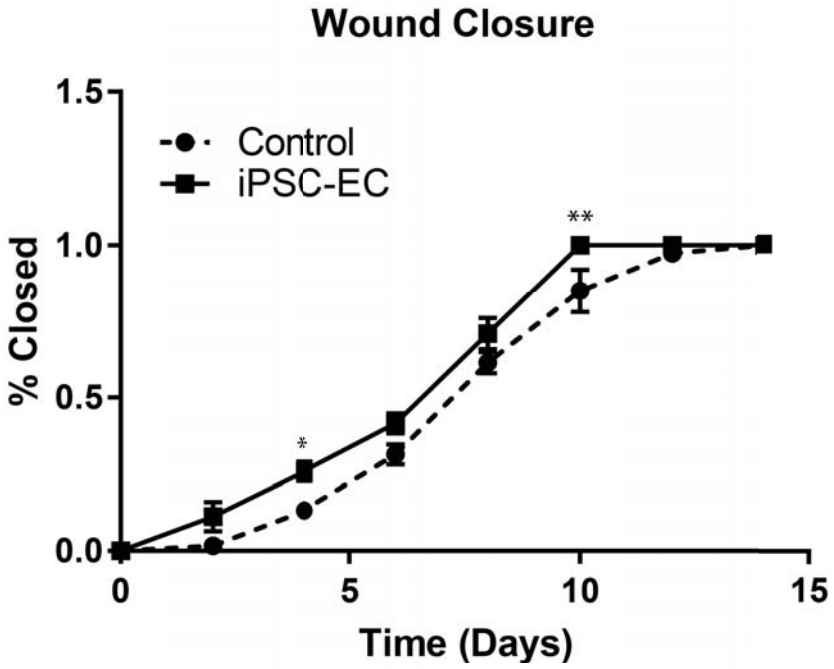
Wound Closure
Control
iPSC-EC
% Closed
Time (Days)
0.0
0.5
1.0
1.5
0
5
10
15
*
**

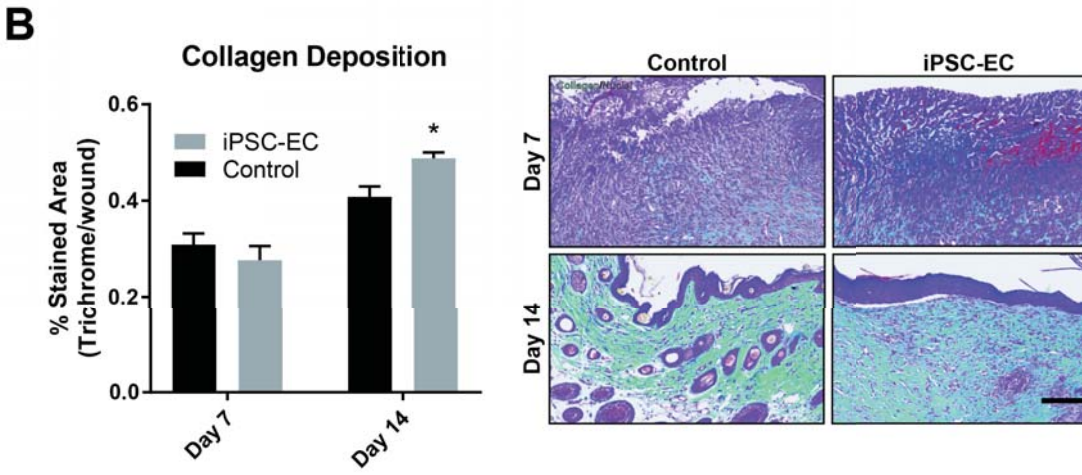
B
Collagen Deposition
% Stained Area
(Trichrome/wound)
iPSC-EC
Control
0.0
0.2
0.4
0.6
Day 7
Day 14
*
Control
iPSC-EC
Day 7
Day 14

Figure 4

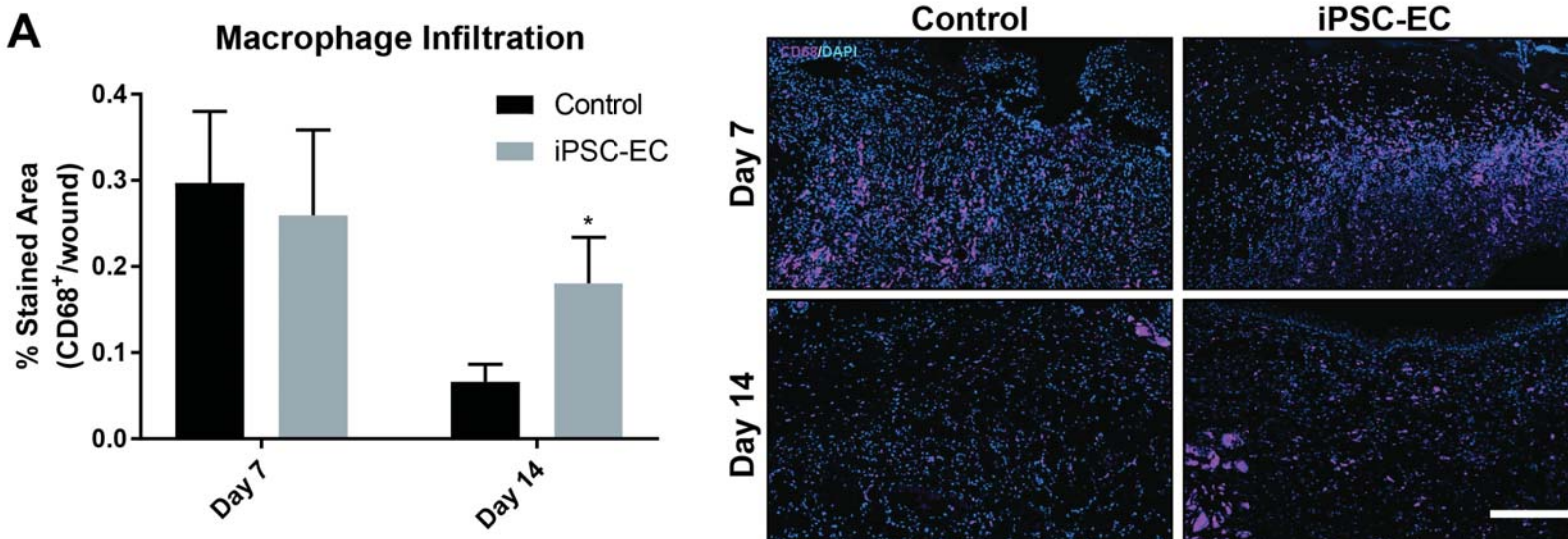
A
Macrophage Infiltration
% Stained Area
(CD68+/wound)
0.4
0.3
0.2
0.1
0.0
Control
iPSC-EC
*
Day 7
Day 14
Control
iPSC-EC
CD68/DAPI
Day 7
Day 14

Figure 5

Dermal fibroblasts

Induced Pluripotency

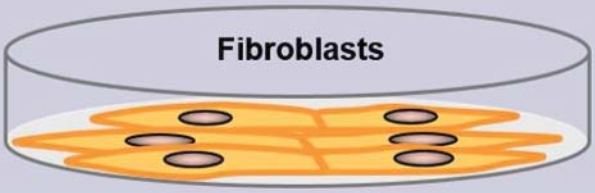

Reprogramming (14 days)

INTEGRATING VECTORS

- Retrovirus (OKSM)

Induced pluripotent stem cells (iPSCs)

Differentiation (14 days)

Differentiation media:

VEGF
bFGF
BMP4
Endothelial growth medium

Lentivirus LV-pUb-Fluc-GFP

Endothelial cells